

1 THE TEST FACILITY DISCO-C

1.1 General layout of the test facility

A schematic diagram of the test facility DISCO-C is shown in figure 1.1, which consists of three major parts, i.e., the pressure vessel, the cavity and the subcompartments. The pressure vessel is a steel pipe with a model of the reactor pressure vessel at its lower end. The cavity is made of a plexiglass cylinder attached to a steel structure that also holds the pressure vessel and eight boxes, which model the four steam generator and the four pump rooms, respectively.

There are two potential flow paths out of the test cavity. The main flow path is the free flow area around the 8 main coolant lines into the pump and steam generator rooms. The other way out of the reactor pit will be through four ventilation openings in the lower part of the cavity leading to the spreading compartment via an annular channel around the pit, and a connecting channel. This second path was closed in all experiments except one. The pump and steam generator rooms are open to the dome in the prototype and open to the atmosphere in the experiment, only covered by filters for the extraction of fog or droplets. The compartments are volumetrically scaled and contain some baffles.

The exact dimensions of the cavity and pressure vessel are shown in Fig.1.1 and in Table 1.1. DISCO models the RPV and RCS without insulation, because it is assumed that the insulation will be eliminated by the first contact with corium. The DISCO-pressure vessel models the volumes of both the reactor cooling system (RCS) and the reactor pressure vessel (RPV). A disk holding 8 pipes (44 mm I.D., 250 mm length) separates the two partial volumes. This arrangement models the main cooling lines with respect to the flow constriction between RCS and RPV. The various diameters inside of the vessel originate from an intended method of the blowdown mechanism. That employed two rupture disks inside the lower part of the vessel. It turned out to lead to unprototypical blowdown characteristics and was therefore replaced by a single rupture disk at the lower head.

The fluids employed are water or a bismuth alloy (MCP-58®, Bi-Pb-Sn-In-alloy, $\rho = 9230 \text{ kg m}^{-3}$, $T_{\text{melt}} = 60^\circ\text{C}$, similar to Wood's metal) instead of corium, and nitrogen or helium instead of steam. The pressure vessel is filled with gas to a pressure slightly lower than the failure pressure of the rupture disk. A small auxiliary pressure vessel (30 liter), filled to a somewhat higher pressure is connected to the main pressure vessel. By opening a valve electro-pneumatically in the line between the two vessels the pressure in the main vessel increases up to the failing pressure of the rupture disk and the blowdown starts. A break wire at the hole gives the signal for closing the valve again and for the time mark $t = 0$. The valve is closed at $t = 70 \text{ ms}$.

The flow path is through the annular space between RPV and cavity wall, through the vessel support structure, and along the main cooling lines into the compartments of the pumps and steam generators. The flow cross section varies from 7 m^2 in the annulus to 6 m^2 at the support structure and 10 m^2 at the cooling pipes. The constriction at the support was modeled by a conical ring, that reduces the annular gap width from 21.75 mm to 10.75 mm. An additional flow cross section is given by 16 holes (26 mm diameter) in the conical ring. In the annular space behind the conical ring liquid is collected in the experiments up to the height of the lower edge of the holes ($0.6 \times 10^{-3} \text{ m}^3$). This space was filled with silicon rubber in some of the later experiments (s. Fig.1.2, left side).

1.2 Basic geometry with central holes

The failure modes investigated in the first series were central holes in the lower head. These holes were closed by a rupture disk, that had an opening diameter larger than the hole diameter. Figure 1.3 shows an example of a 50 mm diameter hole. The rupture disk is scored, which causes the disk to shear along the score lines, providing a full relief opening. The tips of the four blades might hinder a horizontal spreading of the jet. However, a horizontal spreading is not to be expected. The RPV lower head can hold $3.4 \times 10^{-3} \text{ m}^3$ of liquid (liquid height in the hemisphere is 96 mm). This corresponds to 20 m^3 or approximately 160 t of corium. In the experiments with liquid metal a smaller volume of 3100 and 3000 cm^3 was used. When lateral breaches were investigated, even smaller amounts were used, because the focusing effect of the metal layer above the corium pool in the lower head was to be modeled. So the liquid level was just above the upper edge of the breach.

To investigate the effect of different initial liquid pool depths a standpipe was mounted inside the pressure vessel (Fig. 1.4). The standpipe can hold the same amount of liquid as the lower head, but in the outflow we get two distinct stages, first the liquid jet and then the gas jet, without a stage of a two-phase flow in between. That geometry was used by Bertodano et al. Kim et al. and others. Because of the required length of the standpipe the disk separating the RCS from the RPV volume had to be moved up. Therefore two different dimensions are given in figure 1.2 defining the position of the separation plate. This plate has little effect on the blowdown except for the largest breaches.

1.3 Geometry of lateral breaches

Three types of lateral breaches were investigated. The first type are round holes of 25 and 50 mm diameter on the side of the lower head (Fig. 1.5 and 1.6). The inclination of the axis of the holes is 45 degrees. Their center measured at the inside lies 50 mm above the bottom of the calotte. So, the lower edges of the holes at the inside are 41.15 and 32.4 mm above the bottom of the calotte, respectively. The second type is a horizontal slot, that models a partial rip in the lower head, as it might occur with a side-peaked heat flux distribution. The flow cross section is equivalent to a 25 mm hole (Fig. 1.7). The slot is 12.5 mm wide (high, inclined 45 degrees), and 42.5 mm long with a 6.25 mm radius. The lower edge of the slot is 56.1 mm above the bottom of the calotte. These two types of openings were closed by round rupture disks as with the central holes. The third type models the horizontal rip propagating around the circumference of the lower head leaving only a small section attached (Fig.1.8), as it was observed in the lower head failure (LHF) experiments performed at SNL. Here the calotte was a separate part that was held in position by a steel rod from below at its center. The rod penetrated the bottom of the pit through a airtight lead-in hole. At the start of the experiment the rod was released by breaking the bolts that held the rod in place by detonators. The lower head moved down and was stopped by crushing material on the four pedestals. Two different heights of pedestal were used to obtain different flow cross sections.

1.4 Geometry of the cavity

The diameter of the cavity was increased to make room for an extra cylinder, that should trap the liquid mass and prevent the dispersion into the reactor rooms (Fig.1.9). The other change in the cavity geometry deals with the venting openings of

the reactor pit. There are four holes in the lower part of the pit that are connected by a circumferential channel and a tube to an extra compartment modeling the spreading compartment (Fig.1.10).

Table 1.1. Dimensions of the experiment

	Name	diameter [m]	length [m]	area [m²]	volume [m³]
1	Upper pressure vessel (RCS)	0.227	1.240	0.04047	0.050184
2	Lower pressure vessel (RPV)	0.227	0.144	0.04047	0.005828
	space below separator disk	0.217	0.034	0.03698	0.001257
	cone	0.207	0.300	0.03365	0.010096
	cylinder	0.276 - 0.267	0.246	0.00384	0.000944
	annular gap	0.276	0.275	0.05983	0.016453
	lower head (hemisphere)	0.276	0.091		0.003117
	RPV volume				0.037695
	RCS+RPV volume				0.087879
3	Lower cavity	0.342	0.137		0.008399
4	annular space between RPV and cavity	0.342 - 0.2985	0.327	0.021883	0.007155
5	space at RPV support and main cooling lines				0.021134
	Cavity total				0.036688
6	Pump room (each)	0.186	0.940		0.13113
7	steam generator room (each)	0.240	1.615		0.29850
	Melt spreading room	0.320	0.300	0.096	0.11712
	Venting channel	0.0472	0.0472	0.002228	0.003935

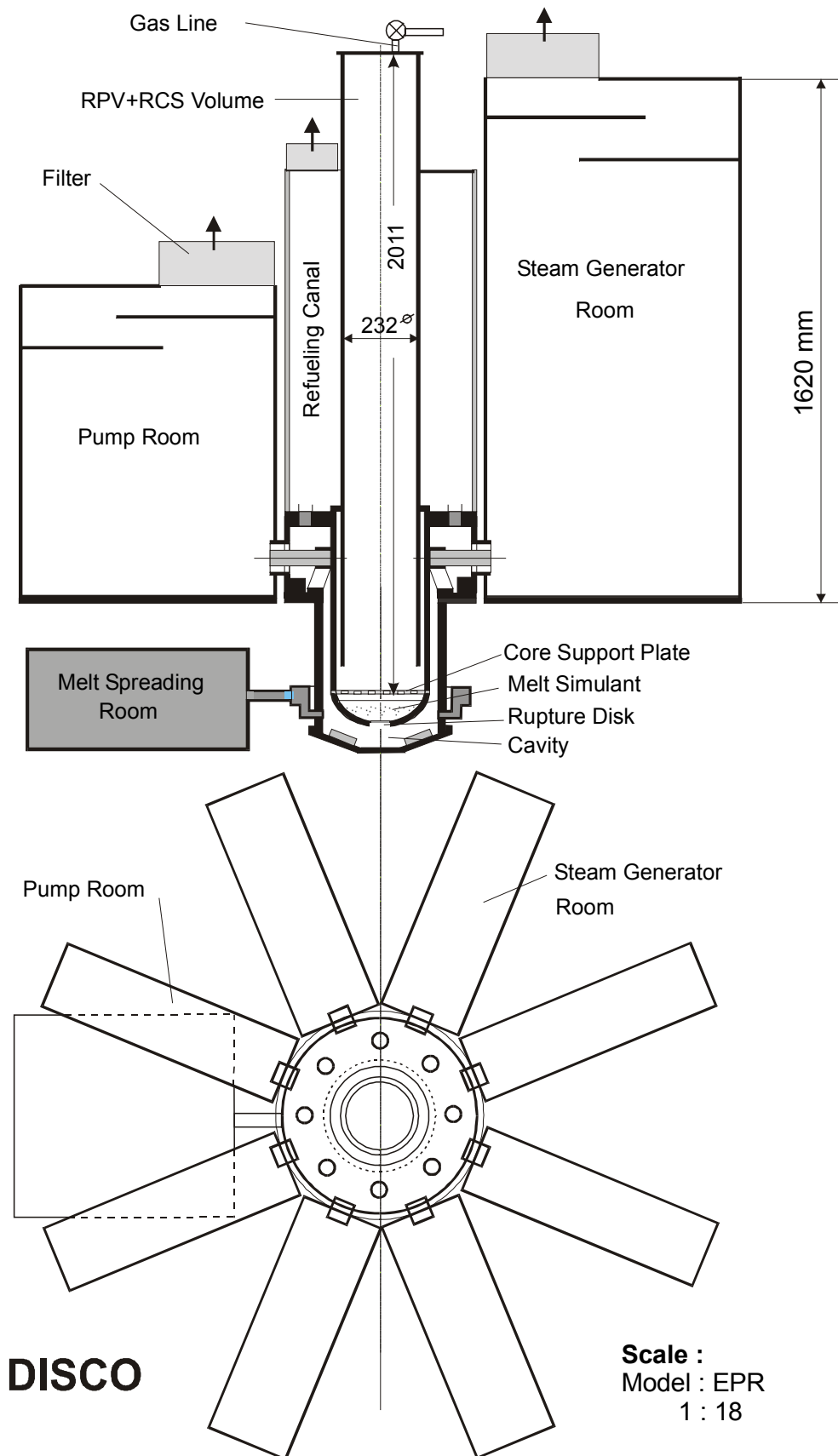


Fig. 1.1 Scheme of the DISCO-C-test facility

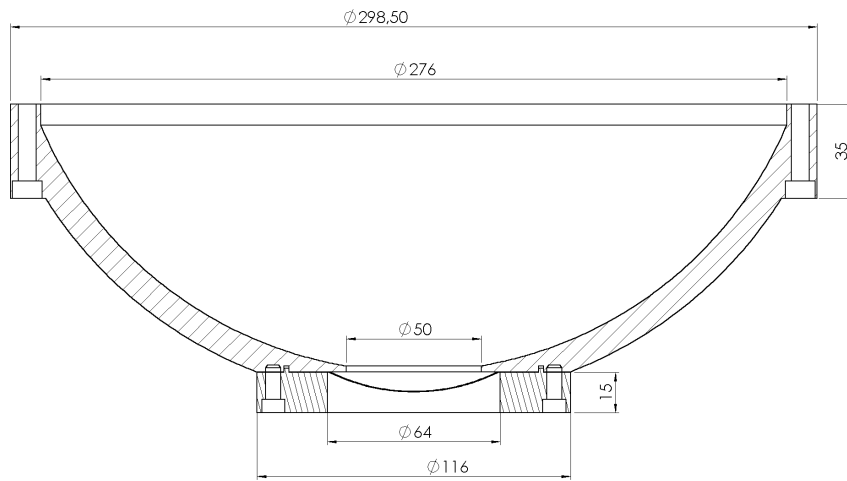
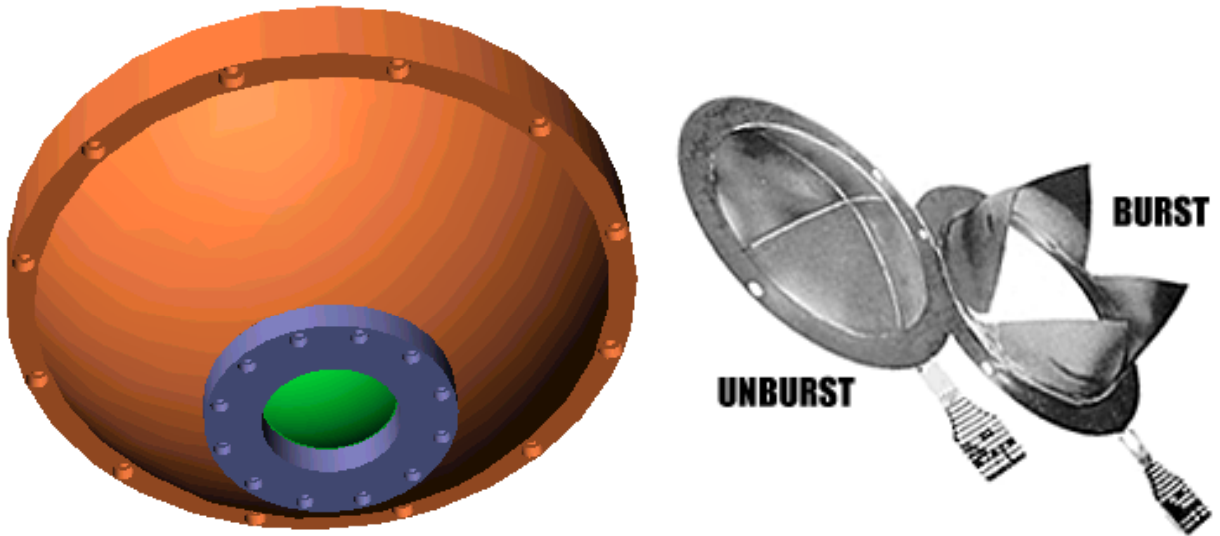


Fig. 1.3 Lower head with central hole and rupture disk

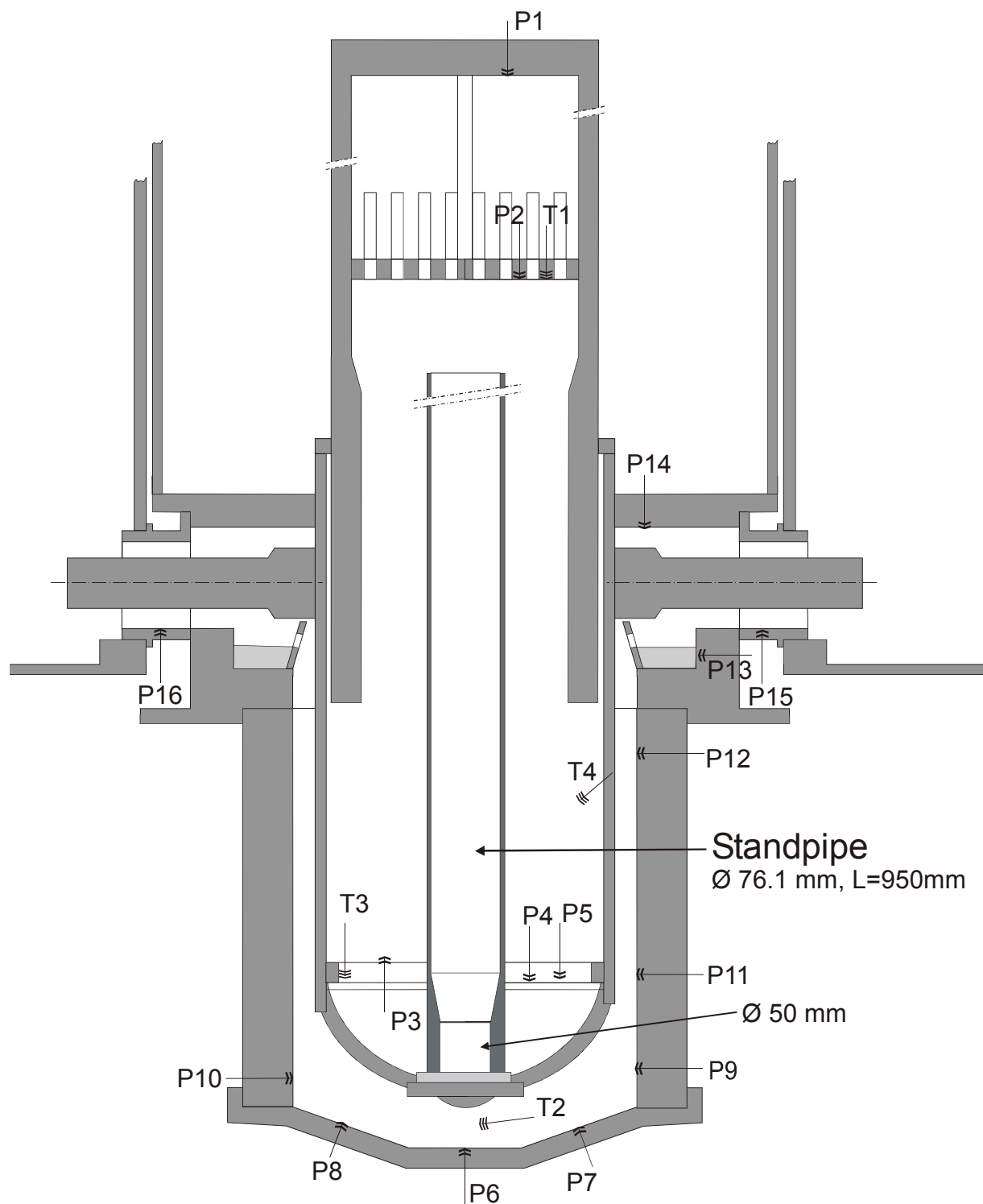


Fig. 1.4 Lower head with standpipe to prevent gas blow through

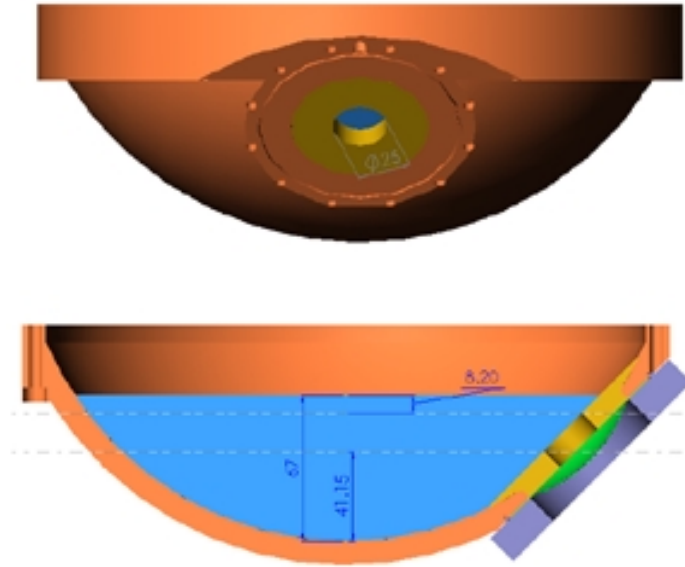


Fig. 1.5. Lower head with lateral hole with 25 mm diameter

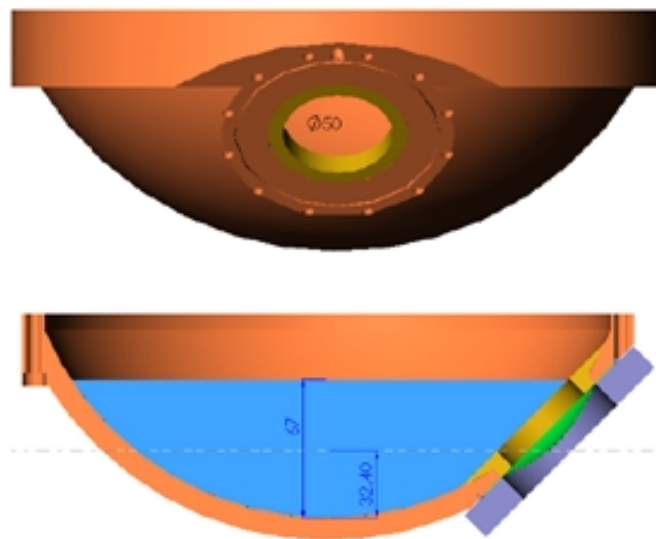


Fig. 1.6. Lower head with lateral hole with 50 mm diameter

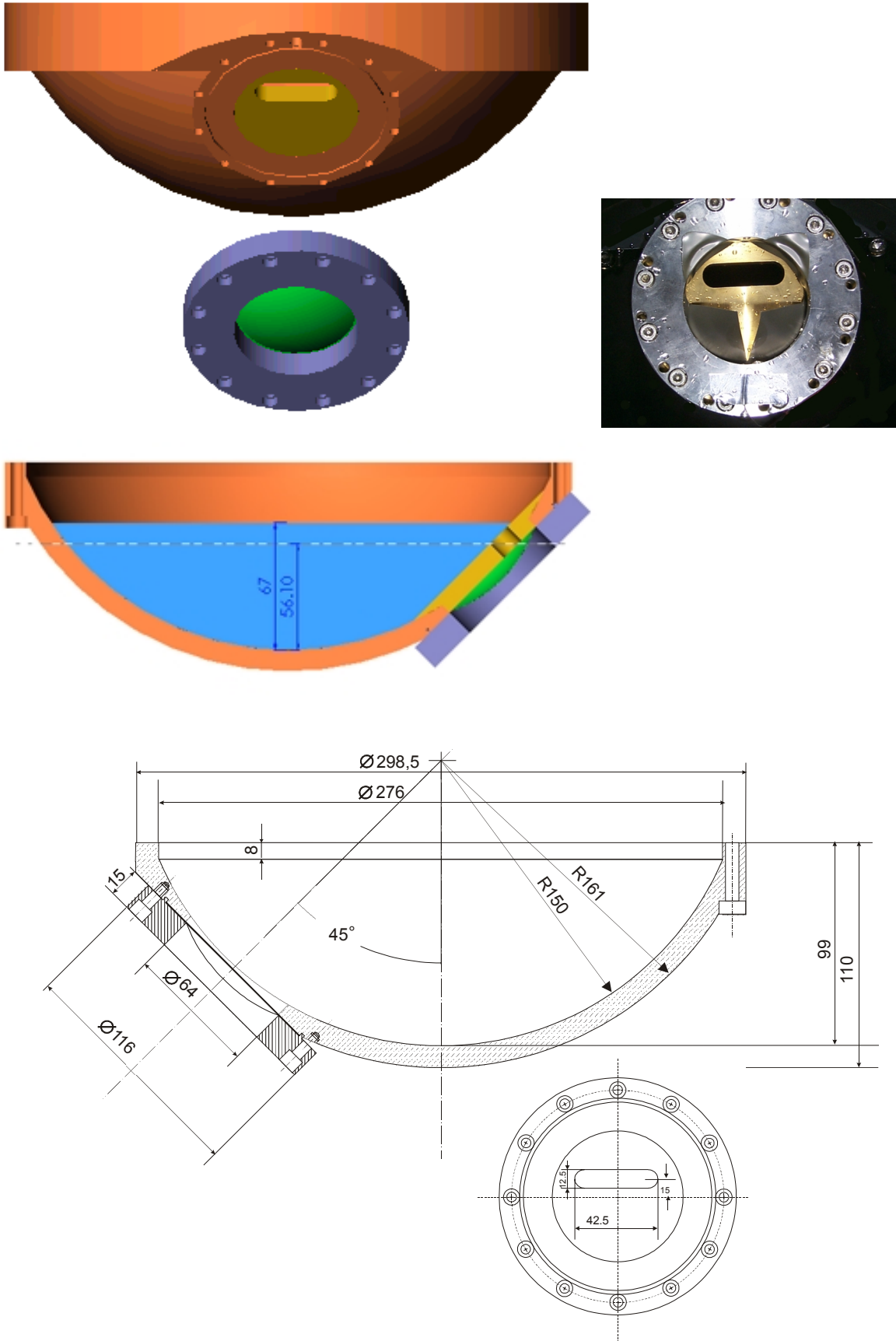


Fig. 1.7. Lower head with lateral slot with a cross section equivalent to a 25 mm diameter hole

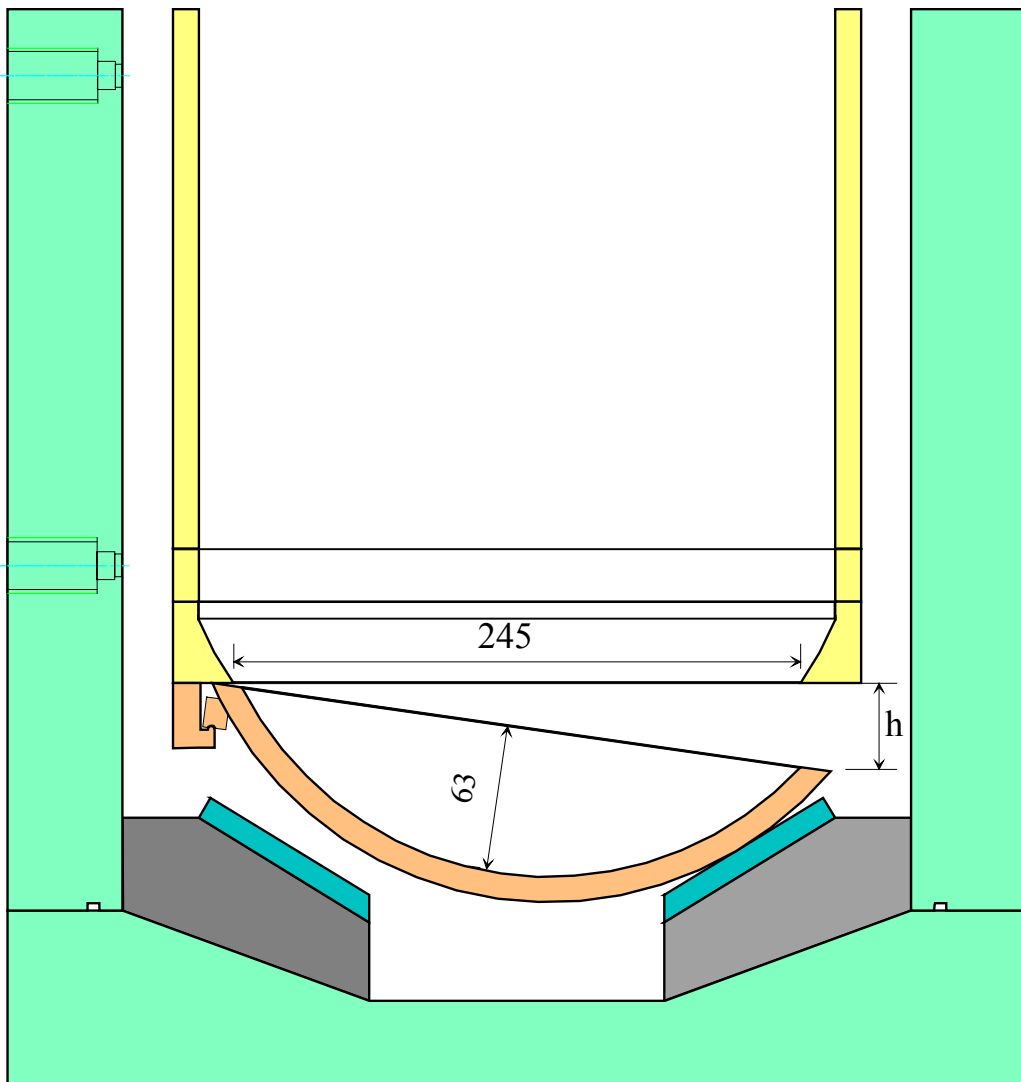


Fig. 1.8. Unzipping and tilting of the lower head

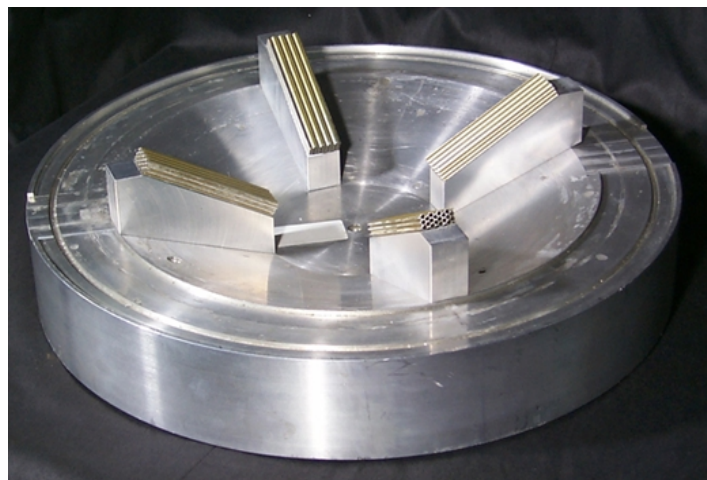


Fig. 1.9. Pedestals to stop the lower head

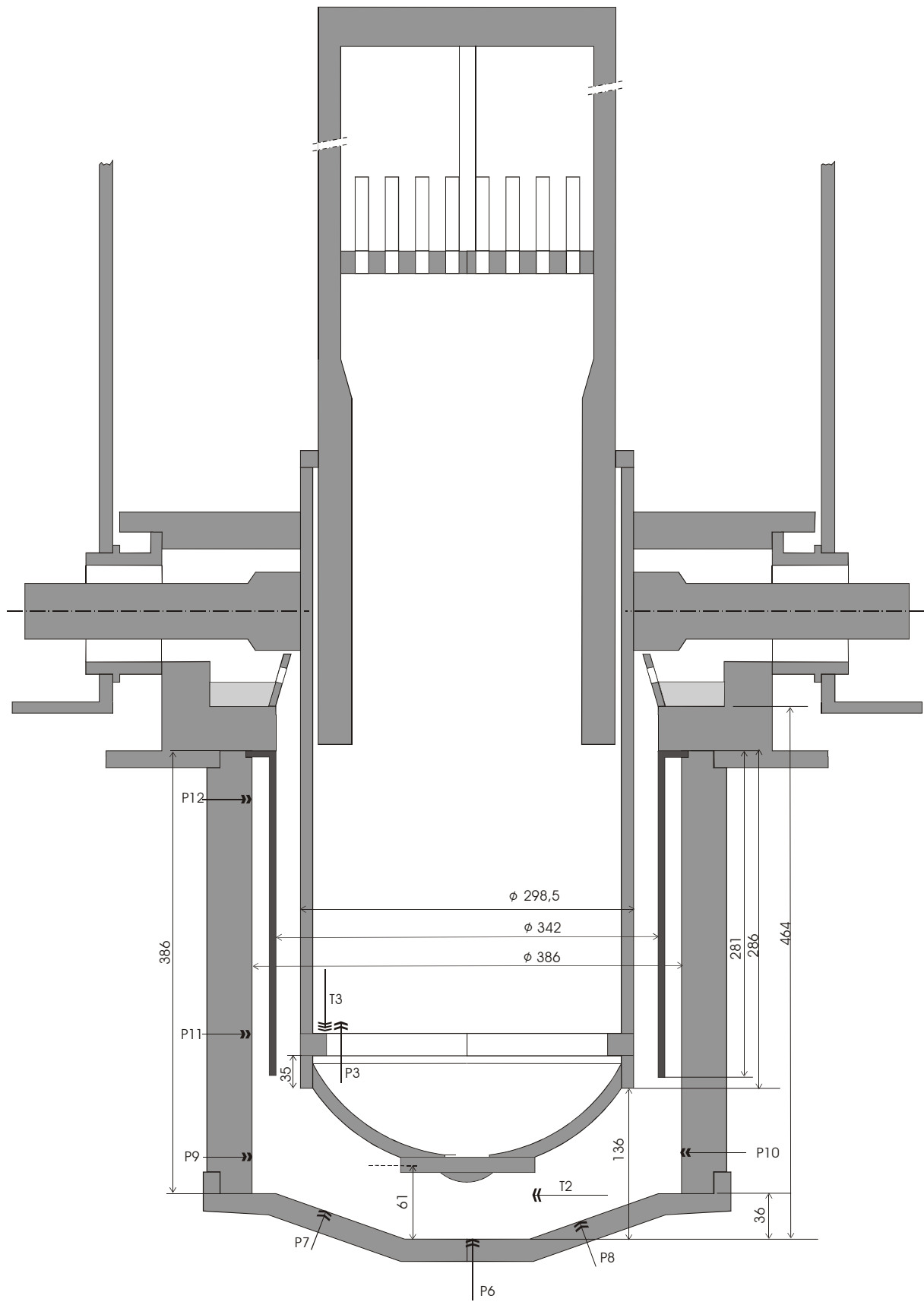


Fig. 1.10. Configuration of the wider cavity with a dispersion preventer device

2 INSTRUMENTATION AND MEASUREMENT

2.1 Pressure Measurement

Transient pressures were measured at the positions indicated in Fig.3 by the marks denoted P1 through P16, and in the subcompartments. Piezo-resistive transducers are used, type Kistler, OEM RES12A, with ranges 2, 5, 10 and 20 bar absolute pressure. The sensors are compensated in the temperature range $-20 \dots +120$ °C. The sensors have a diameter of 12 mm and are mounted in the wall with the steel diaphragm almost flush with the wall. They have a high natural frequency, good linearity and low hysteresis ($\pm 0.3\%$ FSO) and good reproducibility ($< 0.2\%$).

2.2 Temperature Measurement

Although the DISCO-C experiments are not intended to investigate thermal effects, temperatures must be measured because the gas temperature changes during the blowdown and the liquid metal must be heated above the melting temperature of 58°C. Three thermocouples in the pressure vessel and one in the lower cavity measure the gas and liquid temperature (for positions see Fig.3). The K-type thermocouples have a diameter of 0.36 mm. The time constant for gas temperature measurement is between 0.5 s and several seconds, depending on the heat transfer coefficient, with an estimate for our conditions of $0.6 \text{ s} < \tau < 1.2 \text{ s}$. Therefore all temperature signals for gas will be attenuated.

2.3 Gas Velocity Measurement

The velocity of the gas in the annular flow cross section was measured by the Particle Imaging Velocimetry method (PIV) for some selected tests. Tracer particles consisting of oil droplets (with a diameter of approximately 10 μm) were added to the gas in the pressure vessel immediately before the blow down. A region about 30 mm high near the top end of the annular cross section was illuminated by a pulsed laser light sheet through a special window. Perpendicular to the illumination (tangential to the RPV-vessel) a second window was installed in the plexiglass cylinder, through which a camera had a view of the flow cross section (Fig.2.1). A special CCD-video camera recorded 15 double frames per second, shifted in time by 10 to 20 microseconds. With the PIV-software the velocity field of the gas between the two cylinders can be determined.

2.4 Liquid Mass Flow Measurement

For the determination of the liquid mass flow rate through the annular flow cross section a capacitive measurement system was applied. The capacitor consists of a thin metal foil (50 μm thickness, 50 mm vertical, 300 mm horizontal) fixed to the inside wall of the plexiglass cylinder (cavity) and the pressure vessel as the second electrode. The capacitance without liquid between the two electrodes is approximately 27 pF. It depends on how much material lies between the outer probe and the vessel wall. This capacitance is measured by feeding a high frequency voltage at a constant frequency (5,3 V, 33 kHz) to the electrodes. The higher the capacitance of the capacitor, (and therefore the larger the liquid mass) the greater is

the high frequency current flowing through the capacitor. An electronic converts the high frequency current into a frequency proportional to the liquid mass. The electronic unit was originally built for a liquid level meter, that works on the same principle (Endress + Hauser, EC 37Z). Two such probes were used in some experiments in a vertical distance of 50 mm (Positions see Fig.1.2).

2.5 Dispersed Liquid Mass Fraction Measurement

The mass fraction of the water or liquid metal in the compartments was determined by weighing the boxes before and after the test with a precision scale with an uncertainty of ± 0.1 gram. The water in the cavity was absorbed in dry cloth, that was weighed. The metal was solid after the test and could be weighed directly.

2.6 Flow Visualization

Two high speed movie film cameras (LOCAM II, 500 frames/second) are used to record the flow phenomena in the cavity; they are arranged in a view angle of 90 degree to each other. Additionally two CCD-video cameras are taking pictures from the cavity for a quick view. The liquid flow along the cooling pipes into the subcompartments is filmed by a CCD-video camera with high shutter speeds (50 frames/second). For two experiments two subcompartment boxes were removed for a better view and lighting. The exit region was illuminated by a pulsed laser light sheet from above, and a special CCD-video camera recorded 15 double frames per second, shifted in time by 10 to 20 μ -seconds. With the PIV-software (Particle Imaging Velocimetry) the velocity of the liquid and the gas can be determined.

2.7 Data Acquisition and Experiment Control

The pressure and temperature data are acquired by a Data Translation Board DT2839 at a sampling rate of 2.5 kHz. 30 channels for pressure and 4 channels for temperature are currently used. Additionally the signals are recorded from the electro-pneumatic valve (open/closed) and the break wire as a time-zero and sync-signal. A second computer acquires the data from the liquid mass flow measurement with a sampling rate of 35 kHz and the sync-signal. A third computer controls and acquires the PIV-data and images.

The test sequence is as follows: Three video cameras are started manually, the data acquisition systems and the high speed cameras are started by a starter key, two seconds later the signal for opening the valve is given and the rupture disk breaks within 200 ms. The break wire signal closes the valve that is fully closed 70 ms later. The break wire signal also starts a LED-clock and several single light emitting diodes, which can be seen by various cameras.

